

PHYSICS WITH THE LHeC AND THE FCC-eh*

NÉSTOR ARMESTO

on behalf of the LHeC/FCC-eh Study Group

Instituto Galego de Física de Altas Enerxías IGFAE
Universidade de Santiago de Compostela
15782 Santiago de Compostela, Galicia, Spain

*Received 12 April 2023, accepted 14 April 2023,
published online 6 September 2023*

Here, we review the physics programme at the proposed Large Hadron-electron Collider at the High Luminosity Large Hadron Collider, and Future Circular Collider in electron-hadron mode. We consider Quantum Chromodynamics in both electron-proton and electron-nucleus collisions, and Electroweak, Top, Higgs, and Beyond the Standard Model physics. We comment on the synergies with other collision systems, e^+e^- and hadron-hadron, and the physics possibilities with a joint electron-hadron/hadron-hadron detector.

DOI:10.5506/APhysPolBSupp.16.7-A20

1. Introduction

The Large Hadron-electron Collider (LHeC) is the proposal [1–3] of an upgrade of the High Luminosity Large Hadron Collider (HL-LHC) to study electron-hadron/nucleus collisions in the TeV centre-of-mass (CM) energy regime. An Energy Recovery Linac would accelerate electrons to 50 GeV, to collide with the hadron and nucleus HL-LHC beams, reaching instantaneous luminosities $\sim 10^{34}$ and $7 \times 10^{32} \text{ cm}^{-2}\text{s}^{-1}$ and CM energies 1.2 and 0.8 TeV/nucleon in electron-proton (ep) and electron-nucleus (eA), respectively. The same technique can be employed to provide electron-hadron collisions at the High Energy LHC (HE-LHC) [4] or the Future Circular Collider, where this collision mode (FCC-eh) is one of the three considered ones [5, 6]; the respective CM energies are 1.8 and 3.5 TeV. Details of the parameters of these machines can be found in [7]. They will explore a large kinematic region in momentum fraction x times resolution Q^2 in deep inelastic scattering (DIS), see Fig. 1. They will extend the region explored

* Presented at the 29th Cracow Epiphany Conference on *Physics at the Electron-Ion Collider and Future Facilities*, Cracow, Poland, 16–19 January, 2023.

at the Hadron Electron Ring Accelerator (HERA) in ep by a factor of 15 towards smaller x and larger Q^2 (with ~ 1000 times larger luminosity), and 3–4 orders of magnitude compared to presently available DIS data in eA .

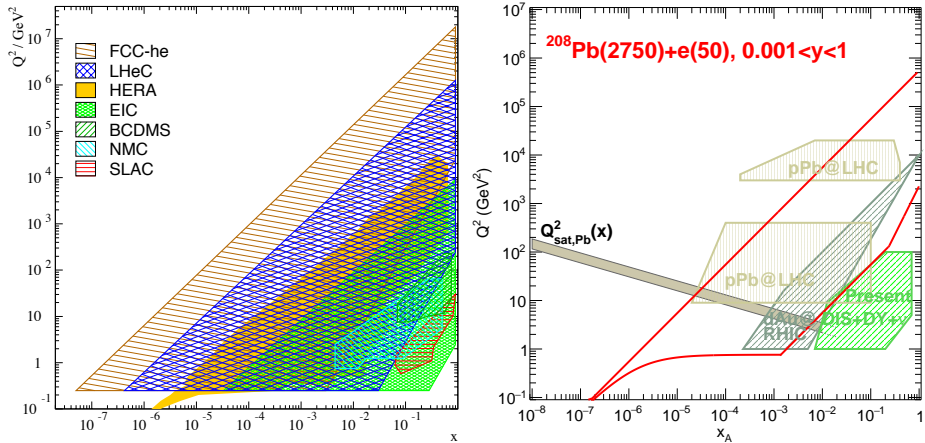


Fig. 1. (Colour on-line) Left: Coverage of the kinematic plane in deep inelastic lepton–proton scattering by some fixed target experiments, with electrons (SLAC) and muons (NMC, BCDMS), and by the ep colliders: the EIC (green), HERA (yellow), the LHeC (blue), and the FCC-he (brown). Taken from [3]. Right: Kinematic plane studied in ePb collisions at the LHeC (solid red/black lines) together with the regions explored in present analyses: DIS and DY fixed target data (hatched area in green), hadron production in dAu collisions at RHIC (hatched area in grey), and Run 1 dijet and EW boson studies in pPb collisions at the LHC (hatched upper region in brown). Also shown in the hatched regions in brown are the coverage from dijets and D -mesons in Run 2 and from EW boson, DY, and photon studies in future runs. Taken from [8].

Here, after a brief presentation of the detector, we review the physics programme that these machines can develop. We consider Quantum Chromodynamics (QCD) in both ep and eA , and Electroweak (EW), Top, Higgs, and Beyond the Standard Model (BSM) physics. We comment on the synergies with other collision systems, e^+e^- and hadron–hadron, and the physics possibilities with a joint electron–hadron/hadron–hadron detector. Due to the limitations of space, only specific examples will be provided. Full details and references can be found in [1, 3–6, 8–12]; see the talk by K. Piotrkowski at [11] for developments in photon physics.

2. Detector

In Fig. 2, we show the present design [8] of the detectors for eh -only mode (asymmetric) and for eh - hh mode (symmetric) for the LHeC. For the central detectors, current acceptances are $|\eta| < 4.7$, which corresponds to one degree angular coverage with respect to the beam pipe. For the FCC-eh, the corresponding detectors would become larger and the acceptance extended to $|\eta| < 6$, see [10, 12]. Additional forward and backward electron and photon taggers, proton spectrometers, and zero-degree calorimeters are not shown. Such a detector would enable the physics programme that is presented in the following sections.

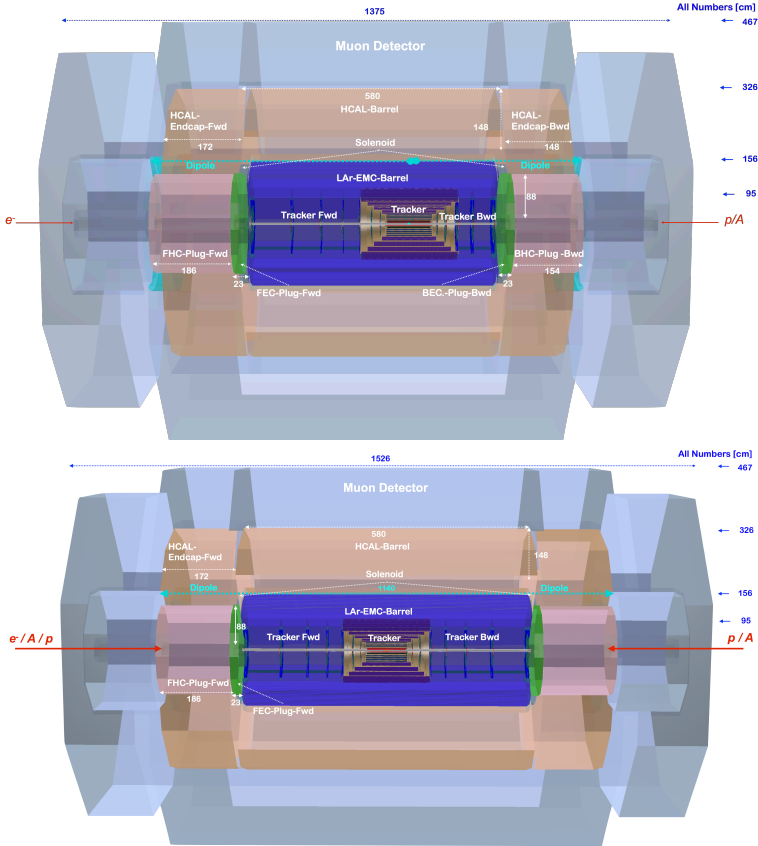


Fig. 2. Designs of the LHeC detector in the eh -only version (top) and in the eh - hh version (bottom). Note the different dimensions and location of the collision point w.r.t. the centre of the LHC interaction point. Taken from [8], see also [10, 12].

3. Physics

3.1. Quantum Chromodynamics

The most basic QCD physics that can be performed with the LHeC and the FCC-eh is the extraction of the collinear parton densities (PDFs) which, through the factorisation theorems, provide the basic ingredients describing hadrons for the prediction of observables with large scales, including EW boson, top and Higgs production, BSM particles, and their respective QCD backgrounds. Therefore, their accurate determination has immediate implications on the physics at hh colliders. At the LHeC and FCC-eh, a precise determination of parton densities is possible, with complete unfolding of all flavour species. Precision will profit from the clean experimental and theoretical environment, with no pileup, small multiplicities compared to hh and many first-principles theoretical calculations available. In a single detector, the standard criterium $\Delta\chi^2 = 1$ for defining Hessian uncertainties in fits can be employed. We refer the reader to [3] for assumptions and details on the generation of the respective pseudodata for neutral (NC) and charged currents (CC), and on the fitting procedure. Note that while the Electron–Ion Collider (EIC) [13] will provide precise data, the larger lever arm in x and Q^2 at the LHeC and FCC-eh will constrain the PDFs in new kinematic regions with abundant access to CC and heavy objects like top quarks.

In Figs. 3 and 4, we show the results of the uncertainties (stemming purely from the experimental aspects) in the extraction of valence and sea quarks and gluons at the LHeC (both in the first run and with full nominal luminosity) compared to existing PDF sets. As seen in those plots, a large precision is already obtained with 50 fb^{-1} integrated luminosity, achievable in the first three years of running. For studies of the impact of different

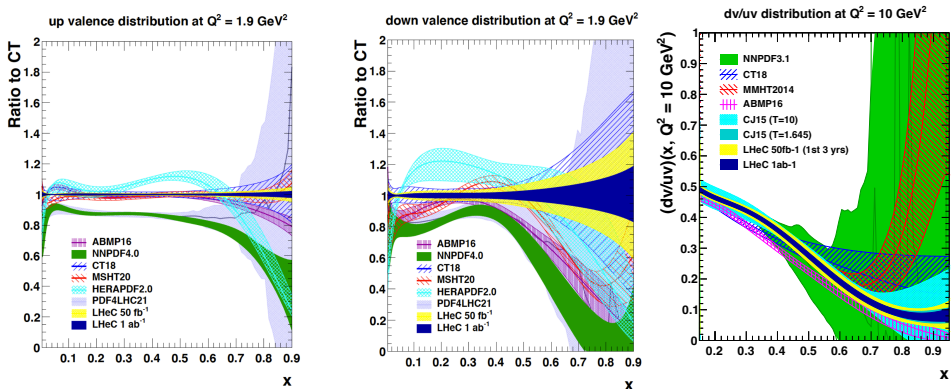


Fig. 3. Distributions (normalised to a given distribution, CT) of up (left) and down (middle) valence quarks, and the ratio d_v/u_v (right), achievable at the LHeC with 50 fb^{-1} and 1 ab^{-1} , compared with existing datasets. See [12].

functional fitting forms and theoretical uncertainties, and of the inclusion of other data sets like heavy quarks, see [3, 9–12]. The impact of LHeC PDFs on parton luminosities for future LHC runs is shown in Fig. 5.

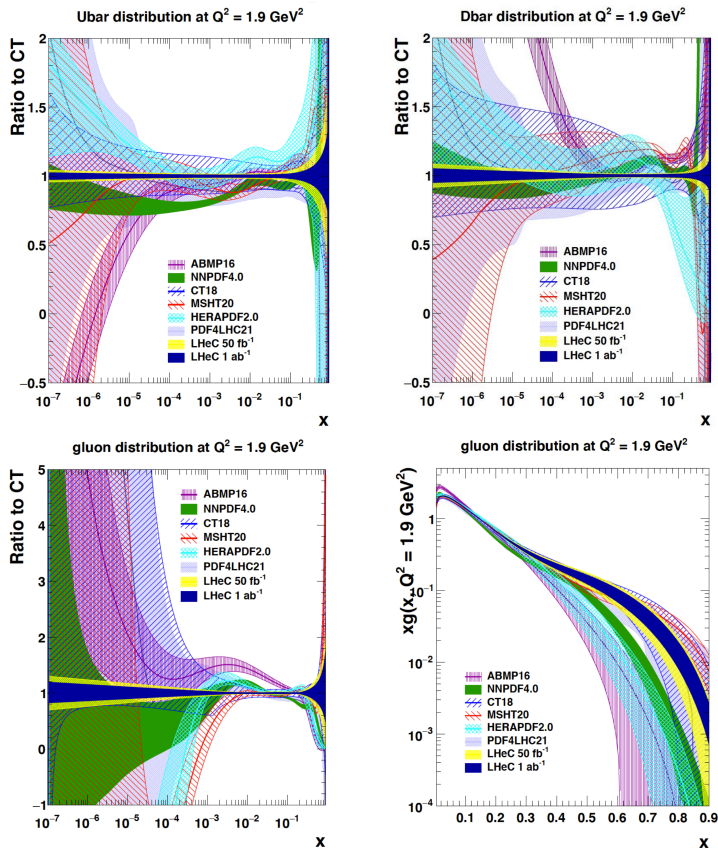


Fig. 4. Distributions (normalised to a given distribution, CT) of up (top left) and down (top right) sea quark and gluons (bottom left) in logarithmic scale, and gluon distribution (bottom right) in linear scale, achievable at the LHeC with 50 fb^{-1} and 1 ab^{-1} , compared with existing datasets. See [12].

In Fig. 6, we show the uncertainties on nuclear PDFs. At the LHeC, the determination of the PDFs of a single nucleus (illustrated by Pb in this figure) will be possible with uncertainties similar to those for the proton. Therefore, there will be no need for nuclear-mass and charge-dependent parametrisation that are currently used due to the scarcity of data for any single nucleus. The question of how the parton structure of a nucleon is affected when immersed in the nuclear medium will be answered quantitatively with large precision in an unprecedented kinematic range.

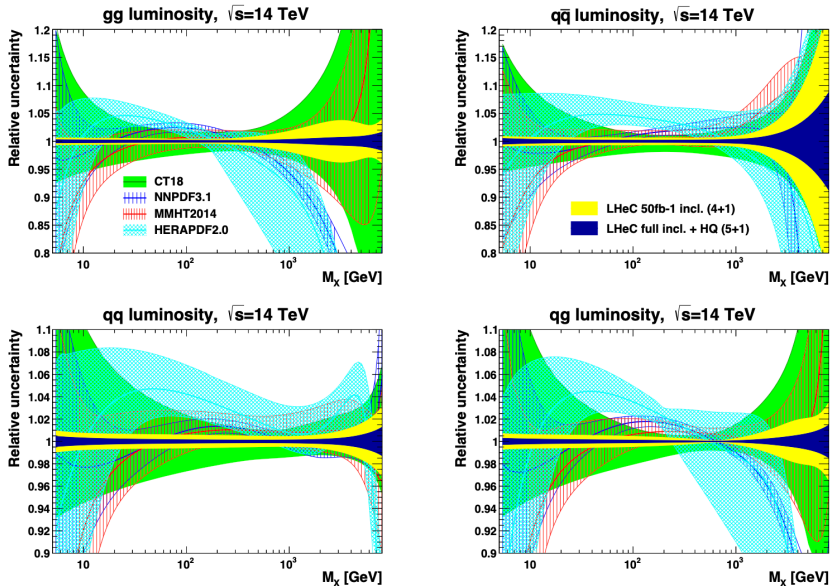


Fig. 5. Relative uncertainties in parton luminosities (gg — top left; $q\bar{q}$ — top right; qq — bottom left; $q\bar{q}$ — bottom right) at $\sqrt{s} = 14$ TeV *versus* the mass of the produced object, M_X , achievable at the LHeC with 50 fb $^{-1}$ and 1 ab $^{-1}$, compared with existing datasets. See [12].

While the studies presented previously make use of NC and CC pseudo-data, full flavour decomposition (by heavy flavour tagging in NC and CC) is not yet used and it is left for the future, together with additional studies on the impact of different functional forms, particularly at small x .

The strong coupling constant α_s is the less precisely determined coupling in the Standard Model (SM). At the LHeC and FCC-eh, accuracies of the order of one per mille are achievable through the simultaneous fit on inclusive cross sections and jets, see Fig. 7. The impact of a more precise determination of PDFs and α_s on EW, Higgs, and BSM physics will be commented below.

While here we have illustrated the most basic QCD aspects that can be studied already at the beginning of the LHeC or FCC-eh operation, many other aspects can be explored that we mention in the following, referring the reader to [1, 3, 8–12] for further details:

- Studies of transverse momentum and generalised parton distributions are possible through the measurement of exclusive diffractive vector meson production and Deeply Virtual Compton Scattering. They will provide three-dimensional information on hadrons and nuclei in kinematic regions not accessible by the EIC.

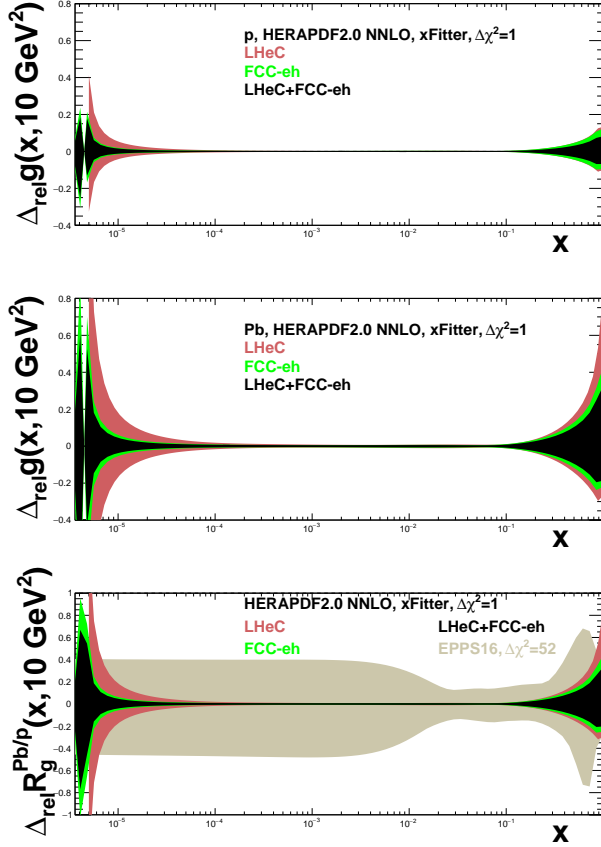


Fig. 6. Uncertainties in the gluon PDF in proton (top) and Pb (middle), and their ratio (bottom), compared to that in a set of nuclear PDFs. Taken from [3].

- Diffractive events, which constitute $\sim 10\%$ of the total DIS cross section at HERA, will be studied in an unprecedented kinematic range, with the possibility of a precise determination of diffractive PDFs of proton and nuclei through measurements of diffractive cross sections and jets, and the diffractive production of heavy objects. Diffractive hard factorisation will be tested in ep and eA .
- The breaking of fixed order perturbation theory (leading to resummation of large logarithms in $1/x$) and the possibility of a novel regime of QCD where parton densities are so large that the linear approximation to QCD radiation fails and non-linear dynamics — leading to the saturation of partonic densities — become dominant, can be cleanly studied in kinematic regimes of relevance for future hadronic colliders. Being a density effect, saturation is enhanced by the increase

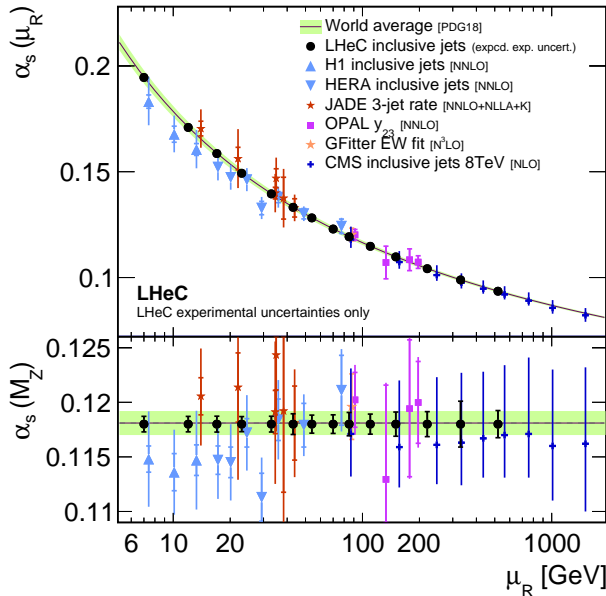


Fig. 7. Illustration of the precision that can be achieved in the extraction of $\alpha_s(M_Z)$ using inclusive jets in DIS at the LHeC. Taken from [3].

of partonic densities towards small x and large nuclear mass number. It is, therefore, essential to study both ep and eA collisions as can be done at the LHeC and FCC-eh. Note that diffraction, which can also be studied in these machines, is expected to be affected by non-linear dynamics. Finally, EW, top, and Higgs physics become small- x physics at the FCC. Large effects on the respective cross sections and backgrounds compared to those computed in fixed order perturbation theory are expected if these new phenomena are at play.

- Other aspects like the relation of diffraction in ep and shadowing in eA , flavour dependence of nuclear antishadowing, \dots , will be accessible at the LHeC and the FCC-eh.

3.2. Electroweak physics

There are numerous EW studies that can be performed with a TeV DIS machine: top, W and Z masses, vector and neutral and charged current couplings to light quarks, the effective mixing angle, \dots , see [3, 9–12, 14]. DIS offers such opportunities in spacelike exchanges, in contrast to the timelike exchanges in e^+e^- and pp . As a first example, in Fig. 8, we show the simultaneous determination of the W mass and Z mass, and the top mass and W mass, through a combined EW+PDF fit with higher-order corrections, in different LHeC scenarios and for different fit assumptions. Determination with

precision comparable or better than previous measurements is possible. In Fig. 9, we show the effective EW mixing angle, which can be extracted with a precision of $\sim 1\%$, together with its running. A simultaneous fit of LHeC and FCC-eh data would allow an extraction with $\Delta \sin^2 \theta_{\text{eff}} = \pm 0.000086$.

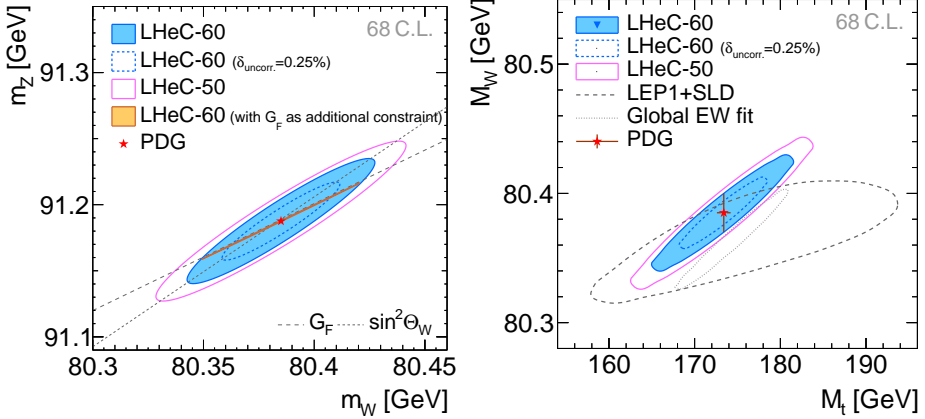


Fig. 8. Simultaneous determination of the top-quark mass M_t and W -boson mass M_W from the LHeC-60 or LHeC-50 data (left). Simultaneous determination of the W -boson and Z -boson masses from the LHeC-60 or LHeC-50 data (right). Taken from [3], see also [14] for explanations and references.

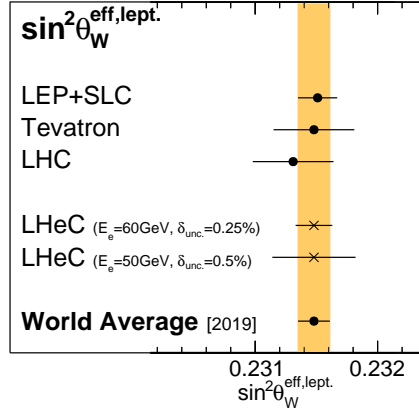


Fig. 9. Comparison of the determination of $\sin^2 \theta_W^{\text{eff,lept.}}(M_Z^2)$ from the LHeC inclusive DIS data with recent averaged values. Results from LEP+SLC, Tevatron, LHC, and the world average value are all obtained from a combination of various separate measurements (not shown individually). For the LHeC, the experimental and PDF uncertainties are displayed. Taken from [3], see also [14] for explanations and references.

Studies performed for the extraction of the W mass indicate that the indirect extraction at the LHeC and FCC-eh could achieve an uncertainty ± 4 MeV. But the role of the LHeC and FCC-eh here goes beyond the indirect determinations that they provide by empowering the physics programme in pp colliders. The LHeC and FCC-eh PDFs, with their much better precision, would allow a reduction in the uncertainties of the determination of several EW parameters at the HL-LHC and FCC-hh. As examples, at the HL-LHC, $\Delta M_W \pm 6$ MeV $\rightarrow \pm 2$ MeV, and $\Delta \sin^2 \theta_{\text{eff}} = \pm 0.00015 \rightarrow \pm 0.00008$, with the use of LHeC PDFs.

3.3. Top physics

At the LHeC and FCC-eh, single-top production in CC and, although with far less statistics, $t\bar{t}$ production in NC, will be studied. Limits on several CKM matrix elements, particularly V_{tb} , can be set using single-top production. For these measurements, electron polarisation, expected to achieve 80%, is essential. Anomalous couplings can be probed, with limits competitive with those at the HL-LHC for the case of the LHeC; also top flavour-changing NC (FCNC, suppressed in the SM and enhanced through BSM) or CP violation in top Yukawa couplings. These facts are illustrated in Figs. 10 and 11.

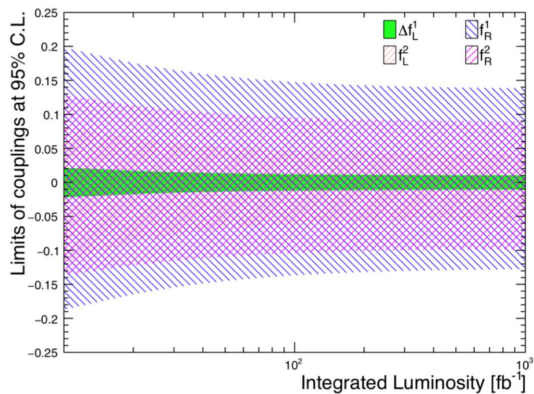


Fig. 10. Expected sensitivities on the SM and anomalous Wtb couplings as a function of the integrated luminosity. Note that in the SM, $f_1^L = 1$ and the other couplings are zero. Taken from [3].

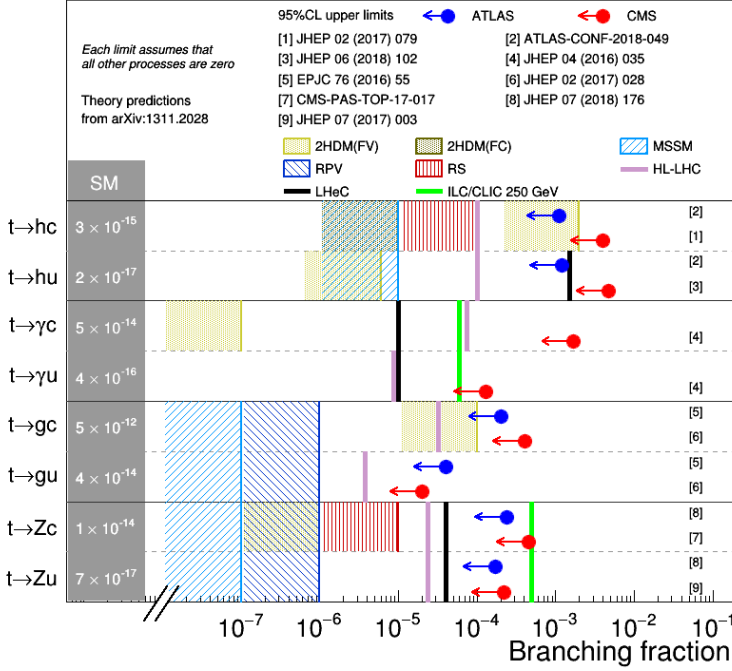


Fig. 11. (Colour on-line) Summary of 95% C.L. limits on top-quark branching fractions in searches for FCNC in top-quark production or decays. The LHeC results (black lines) are compared to current LHC limits (blue/black and red/gray dots), to HL-LHC predictions with 3000 fb^{-1} at $\sqrt{s} = 14 \text{ TeV}$ (magenta/light gray lines), and to predictions from a future ILC collider with 500 fb^{-1} at $\sqrt{s} = 250 \text{ GeV}$ (green/gray lines). The results are also compared to various theory predictions (hatched areas). Taken from [3], where references can be found.

3.4. Higgs physics

At the LHeC and FCC-eh, vector boson fusion (VBF) in NC and CC results in Higgs production. Theoretical predictions at leading order (LO) lead to cross sections 197/24, 372/48, 516/70, and 1038/149 fb in CC/NC at the LHeC, HE-LHeC, low energy FCC-eh and high energy FCC-eh, respectively, with 80% polarisation considered (without polarisation, the numbers for CC/NC are reduced by a factor $\sim 1.8/1.2$). Next-to-leading order corrections are $\sim 20\%$ and produce some shape distortions with respect to LO. Cross sections for double Higgs production are 0.02 and 0.46 fb at the LHeC and FCC-eh respectively.

Such cross sections, of the order or larger than those at e^+e^- colliders, will provide large Higgs datasets for precision measurements. For example, $\sim 10^5$ ($\sim 10^6$) samples are expected in the $b\bar{b}$ channel or ~ 5000 ($\sim 50\,000$) in

the $c\bar{c}$ and ZZ channels, at the LHeC (FCC-eh). The detectors are required large acceptance with heavy flavour identification, $|\eta| < 4.7$ (6) at the LHeC (FCC-eh), to detect the Higgs decay particles. Studies, particularly for the $b\bar{b}$ and $c\bar{c}$ channels, have been done using different techniques and level of sophistication of the detector simulation, and the results shown to be solid against these variations.

In order to illustrate the precision with which Higgs couplings can be measured and how they compare and empower the measurements at hadronic colliders, in Fig. 12 we show the results for the six more frequent Higgs decay channels extracted at the LHeC, the HL-LHC, and the combination of both. Results are shown for the κ parameters which encode the deviations from the SM. It can be observed that ep gives better determinations than pp (with a precision better than 1%) for the $b\bar{b}$, WW , and ZZ channels, and adds $c\bar{c}$ which is defying at the HL-LHC. It also contributes to improvement of all other channels. An SM effective field theory analysis of all couplings in the three collision modes, e^+e^- , pp , and ep , is being carried out which shows that ep adds precision and solves degeneracies in the fit, particularly between the WW and ZZ couplings. We also note that at the FCC-eh, the trilinear Higgs coupling could be determined with a precision of the order of 20%.

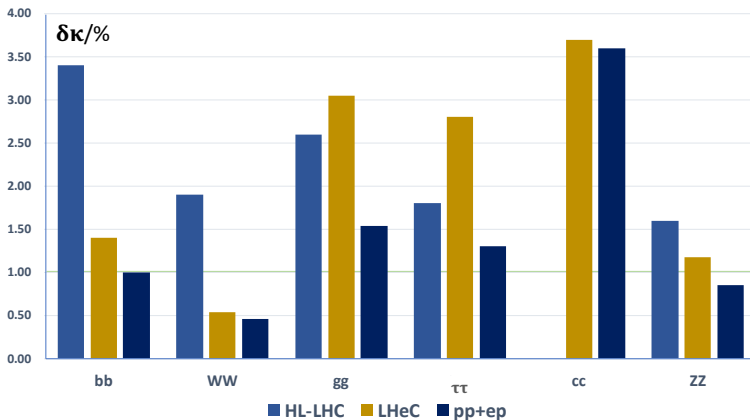


Fig. 12. (Colour on-line) Uncertainty of the determination of the scale factor κ in the measurements of the Higgs couplings, in percent. Only the six most frequent H decay channels are shown. Results are given of the combined HL-LHC+LHeC κ fit (dark blue/black) and of the HL-LHC (blue/gray) and LHeC (gold/light gray) stand-alone fits. There is no accurate measurement expected of κ_c at the LHC. Taken from [3].

Finally, the LHeC will improve the calculation on Higgs cross sections in all production modes by providing more precise PDFs and α_s . This is illustrated in Fig. 13.

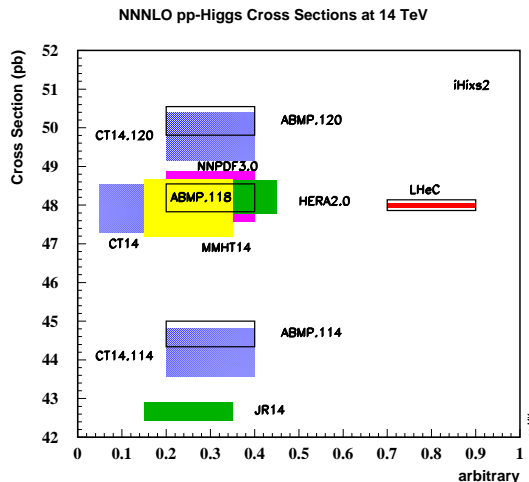


Fig. 13. Cross sections of Higgs production calculated to next-to-next-to-next-to-leading order for existing PDF parameterisation sets (left side) and for the LHeC PDFs (right side). The widths of the areas correspond to the uncertainties as quoted by the various sets, having rescaled the CT14 uncertainties from 90 to 68% C.L. Results (left) are included also for different values of the strong coupling constant $\alpha_s(M_Z^2)$, from 0.114 to 0.120. The inner LHeC uncertainty band (red/thick black) includes the expected systematic uncertainty due to the PDFs, while the outer box illustrates the expected uncertainty resulting from the determination of α_s with the LHeC. Taken from [3] where references can be found.

3.5. Beyond the Standard Model physics

An ep collider is ideal to study common features of electrons and quarks with EW or VBF production, leptoquarks, forward objects, or long-lived particles. With respect to pp , the BSM programme in ep aims to explore new and challenging scenarios and characterise hints for new physics if some excess or deviations from the SM are found at pp colliders.

There exist differences and complementarities with pp colliders. Some promising aspects in ep are the small background due to the absence of QCD interaction between e and p , and the very low pileup. The obvious difficult aspect is the low production rate for new physics processes in ep compared to pp due to the smaller CM energy.

While extensive studies are shown in [1, 3, 5, 6, 8–10, 12], here we mention a few examples. Higgsinos with masses $\mathcal{O}(100)$ GeV appearing in natural SUSY theories can be studied through disappearing tracks, due to the larger sensitivity to very short lifetimes compared to pp colliders. Limits below 5% (1%) can be set on branching ratios of Higgs to invisible (2 scalar long-lived) particles. Dark photons with masses smaller than 1 GeV can be tested via displaced decays into e^+e^- , covering the regions between e^+e^-/pp colliders and low-energy experiments. In Fig. 14, we show the example of sterile neutrinos leading to lepton flavour violation that can be studied through either displaced vertices or trijets.

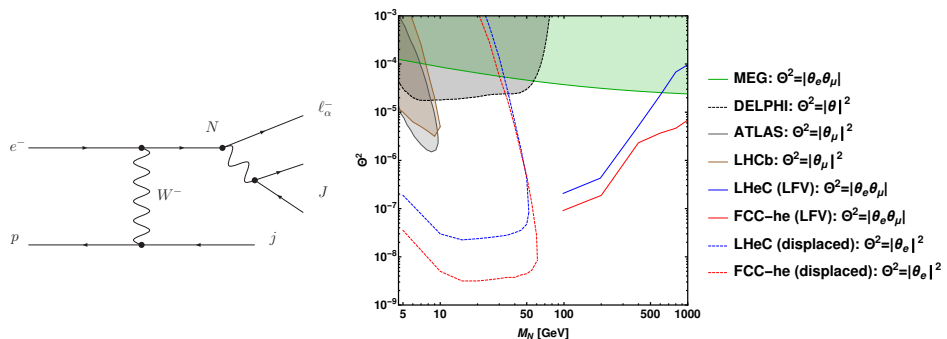


Fig. 14. Left: Dominant tree-level production mechanism for sterile neutrinos at the LHeC. The sterile neutrino decay via the charged current gives rise to the so-called lepton flavour violating lepton-trijet signature. Right: Sensitivity of the LFV lepton-trijet searches (at 95% C.L.) and the displaced vertex searches (at 95% C.L.) compared to the current exclusion limits from ATLAS, LHCb, LEP, and MEG. Taken from [3] where references can be found.

Finally, the improved determination of parton densities at large x at the LHeC and FCC-eh extends the reach of hadronic colliders to larger scales, see [3].

3.6. Physics with a joint eh – hh detector

The possibility of a joint eh – hh interaction region and detector at the HL-LHC, which could be extended to the FCC, was presented in [8–10, 12]. Such a detector, with the excellent calibration that could be achieved in ep , would enhance the possibilities for precision measurements in pp , *e.g.*, W mass measurements with 1 MeV uncertainty.

On the other hand, considering the possibility of studying eA and nucleus–nucleus (AA) collisions in the same apparatus, we note that for AA , eA will provide:

- Knowledge of the nuclear wave function: nuclear PDFs for factorisation tests and precise benchmarking for hard probes to analyse the quark–gluon plasma (QGP), and initial conditions for hydrodynamic evolution to extract transport coefficients of the QGP.
- Knowledge of the dynamics leading to the validity of hydrodynamics which is the main unknown that is addressed in the small system problem — the similarities in many observables measured in pp , $p\text{Pb}$, and PbPb collisions at the LHC.
- Understanding of cold nuclear matter effects on hard probes (*e.g.*, jet quenching or quarkonium).

All these studies will be performed at the EIC but in a kinematic region of much larger values of x than those of relevance for the LHC and future hadronic colliders, which is of particular importance for the first points.

N.A. has received financial support from Xunta de Galicia (Centro singular de investigación de Galicia accreditation 2019–2022, ref. ED421G-2019/05), by European Union ERDF, by the “María de Maeztu” Units of Excellence program MDM2016-0692, and by the Spanish Research State Agency under project PID2020-119632GB-I00. This work has been performed in the framework of the European Research Council project ERC-2018-ADG-835105 YoctoLHC and the MSCA RISE 823947 “Heavy ion collisions: collectivity and precision in saturation physics” (HIEIC), and has received funding from the European Union’s Horizon 2020 research and innovation programme under grant agreement No. 824093. I am most thankful to D. Britzger, J. D’Hondt, M. D’Onofrio, O. Fischer, C. Gwenlan, B. Holzer, M. Klein, U. Klein, P. Kostka, C. Schwanenberger, A. Stasto, and Y. Yamazaki, for comments and help with the talk and proceedings.

REFERENCES

- [1] LHeC Study Group (J.L. Abelleira Fernandez *et al.*), *J. Phys. G: Nucl. Part. Phys.* **39**, 075001 (2012), [arXiv:1206.2913 \[physics.acc-ph\]](#).
- [2] LHeC and PERLE collaborations (O. Brüning, M. Klein), *J. Phys. G: Nucl. Part. Phys.* **46**, 123001 (2019).
- [3] P. Agostini *et al.*, *J. Phys. G: Nucl. Part. Phys.* **48**, 110501 (2021), [arXiv:2007.14491 \[hep-ex\]](#).
- [4] FCC Collaboration (A. Abada *et al.*), *Eur. Phys. J. Spec. Top.* **228**, 1109 (2019).
- [5] FCC Collaboration (A. Abada *et al.*), *Eur. Phys. J. C* **79**, 474 (2019).

- [6] FCC Collaboration (A. Abada *et al.*), *Eur. Phys. J. Spec. Top.* **228**, 755 (2019).
- [7] F. Bordry *et al.*, [arXiv:1810.13022 \[physics.acc-ph\]](#).
- [8] K.D.J. André *et al.*, *Eur. Phys. J. C* **82**, 40 (2022), [arXiv:2201.02436 \[hep-ex\]](#).
- [9] LHeC/FCC-eh talks presented at the 41st International Conference on High Energy Physics (ICHEP 2022), Bologna, Italy, 6–13 July 2022, <https://agenda.infn.it/event/28874/contributions/>; N. Armesto Perez, *PoS (ICHEP2022)*, 492 (2023); B.J. Holzer *et al.*, *PoS (ICHEP2022)*, 057 (2023).
- [10] Electrons for the LHC: LHeC/FCC-eh and PERLE Workshop, IJCLab Orsay, France, 26–28 October 2022, <https://indico.ijclab.in2p3.fr/event/8623/>
- [11] LHeC/FCC-eh talks presented at this conference, 29th Cracow Epiphany Conference on Physics at the Electron–Ion Collider and Future Facilities, Cracow, Poland, 16–19 January, 2023, <https://indico.ifj.edu.pl/event/901/contributions/>
- [12] LHeC/FCC-eh talks presented at DIS2023: XXX International Workshop on Deep-Inelastic Scattering and Related Subjects, Michigan State University, USA, 27–31 March, 2023, <https://indico.cern.ch/event/1199314/contributions/>
- [13] R. Abdul Khalek *et al.*, *Nucl. Phys. A* **1026**, 122447 (2022), [arXiv:2103.05419 \[physics.ins-det\]](#).
- [14] D. Britzger, M. Klein, H. Spiesberger, *Eur. Phys. J. C* **80**, 831 (2020), [arXiv:2007.11799 \[hep-ph\]](#).